H2-dependent formate production by hyperthermophilic Thermococcales: an alternative to sulfur reduction for reducing-equivalents disposal

Sébastien Le Guellec, Elodie Leroy, Damien Courtine, Anne Godfroy, Erwan Roussel

The ISME Journal (2021) 15:3423–3436
https://doi.org/10.1038/s41396-021-01020-x

ARTICLE

H_2-dependent formate production by hyperthermophilic *Thermococcales*: an alternative to sulfur reduction for reducing-equivalents disposal

Sébastien Le Guellec[1] · Elodie Leroy[1] · Damien Courtine[1] · Anne Godfroy[1] · Erwan G. Roussel[1]

Received: 24 November 2020 / Revised: 13 May 2021 / Accepted: 20 May 2021 / Published online: 4 June 2021

Abstract

Removal of reducing equivalents is an essential catabolic process for all microorganisms to maintain their internal redox balance. The electron disposal by chemoorganotrophic *Thermococcales* generates H_2 by proton reduction or H_2S in presence of S^0. Although in the absence of S^0 growth of these (hyper)thermopiles was previously described to be H_2-limited, it remains unclear how *Thermococcales* could be present in H_2-rich S^0-depleted habitats. Here, we report that 12 of the 47 strains tested, distributed among all three orders of *Thermococcales*, could grow without S^0 at 0.8 mM dissolved H_2 and that tolerance to H_2 was always associated with formate production. Two conserved gene clusters coding for a formate hydrogenlyase (FHL) and a putative formate dehydrogenase-NAD(P)H-oxidoreductase were only present in H_2-dependent formate producers, and were both systematically associated with a formate dehydrogenase and a formate transporter. As the reaction involved in this alternative pathway for disposal of reducing equivalents was close to thermodynamic equilibrium, it was strongly controlled by the substrates–products concentration ratio even in the presence of S^0. Moreover, experimental data and thermodynamic modelling also demonstrated that H_2-dependent CO_2 reduction to formate could occur within a large temperature range in contrasted hydrothermal systems, suggesting it could also provide an adaptive advantage.

Introduction

Thermococcales is one of the most ubiquitous hyperthermophilic *Archaea* orders found in hydrothermal ecosystems colonising a wide range of ecological niches such as deep-sea hydrothermal vents or oil reservoirs [1]. *Thermococcales* order is divided into three genera *Thermococcus* [2], *Pyrococcus* [3] and *Palaeococcus* [4] and comprises forty-two type strains and numerous isolates in laboratory and culture collections. They are described as obligate anaerobes and organotrophs utilising peptides or carbohydrates and producing acetate, carbon dioxide (CO_2) and hydrogen sulphide (H_2S)/dihydrogen (H_2) as major end products. Moreover, some carboxidotrophic *Thermococcales* can also oxidise carbon monoxide (CO) to H_2 and CO_2 [5, 6].

Reducing equivalents are disposed either by reduction of elemental sulfur (S^0) to H_2S or in its absence by proton reduction to H_2. In both cases, an electrochemical sodium ion gradient is generated driving the synthesis of ATP by a Na^+-dependent ATP synthase [7, 8]. The sulfur-dependent metabolic switch is controlled by the transcription factor SurR in response to the S^0 availability [9–11]. Thus, in the presence of S^0 or polysulphide (e.g., [12]), a membrane-bound sulfane reductase complex (MBS, previously described as MBX) is transcribed leading to the generation of H_2S [13], whereas transcription of a membrane-bound ferredoxin (Fd)-oxidising hydrogenase complex (MBH) responsible for H_2 production is not induced [14, 15]. Inversely, in the absence of S^0 only the transcription of the Mbh complex is activated. In this case and without interspecies H_2 transfer [16], endogenous or environmental H_2 accumulation inhibits growth of *Thermococcales* by blocking the recycling of the reduced ferredoxin pool [17, 18]. However, some *Thermococcales* have been shown to tolerate H_2 in the absence of S^0 as several have been isolated in the presence of H_2 (e.g., *Thermococcus piezophilus* $CDGS^T$ [19]).

Supplementary information The online version contains supplementary material available at https://doi.org/10.1038/s41396-021-01020-x.

✉ Erwan G. Roussel
Erwan.Roussel@ifremer.fr

[1] Ifremer, Univ Brest, CNRS, Laboratoire de Microbiologie des Environnements Extrêmes, Plouzané, France

A recent transcriptomic study suggests that *Thermococcus paralvinellae* ES1^T could dispose of the excess electrons through H_2 oxidation to formate using Formate hydrogenlyase (FHL) complex encoded by the *fdh-mfh-mnh* cluster [20]. Although FHL was initially described as responsible for formate oxidation to H_2 and CO_2 ($HCOO^- + H_2O \rightarrow H_2 + HCO_3^-$) coupled to ATP synthesis for *Thermococcus onnurineus* NA1 in pure culture conditions [21–23], it remains unclear whether the cells only rely on formate or if the relatively high amounts of yeast extract present in the medium could also sustain the anabolism [24]. However, some formate dehydrogenases (FDH) are also known to catalyse both reactions, oxidation of formate and reduction of CO_2 [25–27].

Owing to the small Gibbs free energy change in standard conditions ($\Delta G° = +1.3\ kJ\ mol^{-1}$), the direction of the reaction is primarily thermodynamically controlled by the concentration of reagents. However, it still remains unclear what reaction is catalysed in situ by *Thermococcales* [20]. The aim of this study is to characterise the reaction catalysed by formate dehydrogenase (H_2-dependent formate production and/or formate oxidation) in hyperthermophilic *Thermococcales* and to determine its in situ physiological role.

Materials and methods

Strain collections

All *Thermococcales* strains used in this study were obtained from the Laboratory of Microbiology of the Extreme Environments microorganisms collection (Ifremer, Plouzané, France), the Université de Bretagne Occidentale Culture Collection (UBOCC, Plouzané, France), the German Collection of Microorganisms and Cell Cultures (DSMZ, Braunschweig, Germany) and the Japan Collection of Microorganisms (JCM, Wako, Japan) (for details, see Table S1). *Thermococcus nautili* 30-1^T was kindly provided by Dr. A. Gorlas (Institut de Biologie Intégrative de la Cellule, Orsay, France). *Thermococcus* sp. MF15 was isolated from samples collected from the Snake Pit hydrothermal field during cruise BICOSE 2014 [28].

Culture conditions

Thermococcales were grown under anaerobic conditions in an artificial seawater medium (ASW) containing the following components in $g\ L^{-1}$: NaCl (27.2), $MgCl_2{\cdot}6H_2O$ (10.0), $CaCl_2{\cdot}2H_2O$ (1.5), KCl (0.66), KBr (0.1), H_3BO_3 (0.025), $SrCl_2{\cdot}6H_2O$ (0.04) NH_4Cl (0.021), KH_2PO_4 (0.0054) and NaF (0.003). The medium was supplemented with $1\ mL\ L^{-1}$ of trace-element solution SL 10 [29] and $0.2\ mL\ L^{-1}$ of selenite tungstate solution [30]. After autoclaving at 121 °C during 60 min, the medium was cooled under an atmosphere of N_2/CO_2 (80:20, v/v; 30 kPa), prior to the addition of sodium bicarbonate solution from a sterile stock solution at the desired concentration. The medium was reduced with $1.2\ mL\ L^{-1}$ of sodium sulphide ($Na_2S{\cdot}9H_2O$) at 1 M and the pH was adjusted at 6.8 by the addition of sterile HCl from 1 M sterile stock solution. Then, 50 mL medium was transferred under nitrogen flow into 120 mL serum bottles hermetically sealed with butyl rubber septa.

Colloidal sulfur (Sigma Aldrich, St. Louis, MO, USA) and yeast extract (Fisher Scientific, Hampton, NH, USA) were added at a constant volume ratio of 1% (v/v) in serum bottles at a desired final concentration from sterile stock solutions. Serum bottles were flushed and pressurised (200 kPa at 80 °C) with the desired gas phase consisting of $H_2/N_2/CO_2$ (CO_2 was kept constant in the gas phase at 20%).

Unless otherwise indicated, each experiment was carried out in triplicate and incubated at 80 °C (optimal growth temperature of *T. onnurineus* NA1 [31]) in unshaken static conditions. Inoculation was always performed at 1% (v/v) from exponential phase cell cultivated on ASW with $2\ g\ L^{-1}$ yeast extract and with N_2/CO_2 (80:20; v/v; 200 kPa) as gas phase. Cells were observed under an Olympus BX60 phase-contrast microscope (Olympus Corporation, Tokyo, Japan). Cell quantification was assessed by direct cell counting using a Thoma cell counting chamber (depth 0.02 mm).

Volatile fatty-acid analysis

Formate and acetate concentrations were determined using a Dionex ICS-2000 Reagent-Free Ion Chromatography System equipped with an AS50 autosampler (Thermo Fisher Scientific, Waltham, MA, USA) as described by Roussel et al. [32]. Chromatographic separation was conducted on two Ionpac AS15 columns (4 × 250 mm) at 30 °C and the determination of species was carried out using an anion self-regenerating suppressor (ASRS 300 4-mm) unit in combination with a DS6 heated conductivity cell (35 °C). The gradient programme was as follows: 8 mM KOH (29.9 min), increase 28.5 mM KOH min^{-1} to 65 mM (30.1 min), decrease 57 mM KOH min^{-1} to 8 mM (9 min). Prior to ion chromatographic analysis, 0.5 mL of culture was sampled and then centrifuged (15 min at 12,000 × *g* at room temperature). The supernatant was diluted (1:10, v/v) in ultrapure water (Millipore, Billerica, MA, USA).

^{14}C-radiolabelled formate measurements

H_2-dependent formate production from bicarbonate was measured using ^{14}C-radiolabelled substrate. Culture conditions were identical as previously described. *T.*

onnurineus NA1 was cultivated in 50 mL ASW medium supplemented with 0.2 g L^{-1} of yeast extract and 30 mM bicarbonate, without S^0 and pressurised with H_2/CO_2 or N_2/CO_2 (80:20, v/v; 200 kPa). [^{14}C]Na-HCO_3^- with a specific activity of 59.0 mCi $mmol^{-1}$ was purchased from Perkin Elmer (Waltham, MA, USA). Cultures were amended with 28 µL of [^{14}C]Na-HCO_3^- to a final activity of 96 kBq using a Hamilton syringe. Abiotic controls were not inoculated and negative control experiments were performed by autoclaving inoculated cultures (20 min at 121 °C). Each activity measurement for each time point was performed in triplicate. Production of ^{14}C-formate was measured by collection of the ^{14}C-formate fraction using a Dionex ICS-2000 Ion Chromatography System equipped with an AFC-3000 Automated Fraction Collector (Thermo Fisher Scientific, Waltham, MA, USA). All analytical conditions were identical to those described previously for anion analysis. Samples were transferred to OptiPhase HiSafe 3 scintillation cocktail (Perkin Elmer, Waltham, MA, USA) and quantification of ^{14}C-formate was determined by liquid scintillation counting with a Tri-Carb 2910TR liquid scintillation counter (Perkin Elmer, Waltham, MA, USA).

Phylogenomic analysis

A phylogenomic tree was constructed with all *Thermococcales* genomes retrieved from the NCBI genome database (https://www.ncbi.nlm.nih.gov/genome) using a set of 59 conserved phylogenetic marker proteins (Table S2) [33]. Sequences from three *Methanococcus* genomes (*M. aeolicus*, NC_009635.1; *M. vannielii*, NC_009634.1 and *M. voltae*, NC_014222.1) were used as out-group. For each protein, sequences were aligned using MAFFT v7.055b (parameter 'linsi') [34] and alignments were trimmed using BMGE v1.12 (default parameters) [35]. All alignments were then concatenated, and conserved positions across all genomes were removed with Seaview v4.6 [36]. The phylogenomic tree was computed with PhyML v3 [37] on the ATGC Montpellier Bioinformatics webserver (http://www.atgc-montpellier.fr). Model selection was done with SMS [38] using Akaike information criterion. The best model used for the tree was 'LG' [39].

Comparative genomic analysis was performed using EDGAR 1.3 software framework (http://edgar.computational.bio.uni-giessen.de) [40]. Homology searches were conducted with BLASTp using default settings (http://blast.ncbi.nlm.nih.gov/Blast.cgi). Studies of synteny of genes were performed using the SyntTax software (http://archaea.u-psud.fr/synttax) using default parameters [41].

Thermodynamic calculations

Standard Gibbs free energies (ΔG^0) of the reaction of formate production at 25 °C:

$$H_2(g) + HCO_3^-(aq) \leftrightarrow HCOO^-(aq) + H_2O(l)$$

were calculated according to:

$$\Delta G^0 = \Delta fH^\circ - T.\Delta S^\circ$$

Where ΔfH° is the standard enthalpy of formation, T the absolute temperature (K) and ΔS° the standard entropy change. Thermodynamic data of reactants and products for species were obtained from the NBS tables of chemical thermodynamic properties [42]. Bicarbonate and formate were assumed as dissolved species. In order to strengthen the demonstration, H_2 was assumed as a gaseous substrate, as the Gibbs free energies of the reaction under non-standard conditions (ΔG') for CO_2 reduction to formate were less favourable than assuming H_2 as dissolved.

The Gibbs free energies of reactions under non-standard conditions ($\Delta G'$) were calculated according to

$$\Delta G' = \Delta G^0 + RT.\ln \mathrm{Qr}$$

Where Qr is the reaction quotient (expressed as concentrations) considering activities almost equal to concentrations based on Amend and LaRowe 2019 [43] (see Supplementary Methods section), R the gas constant (8.314×10^{-3} kJ mol^{-1} K^{-1}) and T the absolute temperature (K).

Arrhenius parameters

An estimation of the temperature dependence of each studied metabolic process could be obtained by calculating the activation energy (Ea) and the Q_{10} factor from Arrhenius plots [44]. The Arrhenius profiles were obtained by plotting the natural logarithm of each maximum rate for each incubation temperature versus the inverse of temperature. The activation energy for each metabolic process was calculated from the following equation:

$$\ln(k) = \ln(A) + \left(\frac{-Ea}{R} \cdot \frac{1}{T}\right)$$

Where Ea is the activation energy (kJ mol^{-1}), k the reaction rate (µmol cm^{-3} day^{-1}), A the Arrhenius constant, R the gas constant (8.314×10^{-3} kJ mol^{-1} K^{-1}), and T the absolute temperature (K).

Q_{10} is the factor by which the rate of reaction increases with a temperature increase of 10 °C. The selected

temperature range in this study was between 75 °C and 85 °C. Q_{10} was calculated using the following equation:

$$Q_{10} = \exp\left[\frac{Ea \cdot 10}{RT(T+10)}\right]$$

Dissolved H_2 concentration determination

Dissolved H_2 concentrations estimated as if they were at equilibrium with the overlying gas phase were calculated according to the Bunsen gas solubility coefficient [45, 46] and Henry's Law:

$$[H_2]_{(aq)} = \frac{P_{H_2} \times \beta}{R \times T}$$

Where $[H_2]_{(aq)}$ is the dissolved H_2 concentration (mol L^{-1}), P_{H_2} the partial pressure of H_2 in the headspace (atm) at the temperature of measurement, β the Bunsen solubility coefficient (0,015022), T the temperature of measurement (353.15 K) and R the gas constant (0.08206 atm L mol^{-1} K^{-1}).

The Bunsen solubility coefficient (β) is expressed as cm^3 of gas STP per cm^3 of water at the temperature of measurement when the partial pressure of gas (gas volume corrected to STP, 0 °C and 1 atm) above the water is 1 atm. According to Weiss [46], it can be expressed as a function of temperature and salinity as follows:

$$\ln\beta = A_1 + A_2\left(\frac{100}{T}\right) + A_3\ln\left(\frac{T}{100}\right) + S‰\left[B_1 + B_2\left(\frac{T}{100}\right) + B_3\left(\left(\frac{T}{100}\right)^2\right)\right]$$

where the A's and B's are constants from Wiesenburg and Guinasso [45] (for this study: $A_1 = -47{,}8948$; $A_2 = 65{,}0368$; $A_3 = 20{,}1709$; $B_1 = -0{,}082225$; $B_2 = 0{,}049564$ and $B_3 = -0{,}0078689$), T is temperature of measurement (353.15 K) and S‰ is salinity (31,860 g kg^{-1}).

Unless otherwise indicated, serum bottles were pressurised with 200 kPa of H_2/CO_2 (80:20, v/v) at 80 °C, which correspond to a calculated dissolved H_2 concentration of 0.8 mM.

Results and discussion

Growth in the absence of S^0 and distribution of H_2-dependent formate production among *Thermococcales*

In order to investigate the inhibition of cell growth by H_2 in the absence of S^0, 47 *Thermococcales* strains were tested in the presence of H_2 in gas phase (80% at 200 kPa; dissolved H_2 concentration 0.8 mM) (Table S1). Twelve strains (26%) that presented significant growth were systematically associated with production of formate (1–12 mM), whereas 35 strains (74%) did not show either of these traits (Fig. 1). The ability to produce formate was evenly distributed across *Thermococcales* order (9 *Thermococcus*, 2 *Pyrococcus* and 1 *Palaeococcus)* with no clear distribution pattern. However, this distribution might be biased as solely relying on the study of species mostly isolated on S^0 rich media. Growth temperatures were also distributed over a large range (50–112 °C) with an average optimal growth temperature of 86 °C, suggesting H_2-dependent formate production could occur over a wide range of microhabitats.

Mainly based on Fiala's pioneering work on *Pyrococcus furiosus* Vc1^T [3, 17], growth of *Thermococcales* is usually described as being inhibited by H_2 accumulation in the absence of S^0. However, our study shows that at least more than a quarter of *Thermococcales* strains tested were tolerant to H_2 in the absence of S^0 and this proportion could be underestimated as most strains capable of formate production were isolated from environments presenting relatively high H_2 concentrations. For example, *T. piezophilus* CDGS^T was isolated from the Piccard hydrothermal vent field (4964 m) that exhibits the highest H_2 concentration measured so far (19.9 mM) in high-temperature hydrothermal fluid [19, 47]. Moreover, with the exception of *T. kodakarensis* KOD1^T isolated from a shallow solfatara on the shore of Kodakara Island, all these strains were also isolated among a wide range of deep-sea hydrothermal vent fields that are characterized by relatively low S^0 (< 33 µM) and polysulfide (0.27 µM) concentrations [48–50], suggesting H_2-dependent formate production would also provide an adaptive advantage.

Genomic comparison

Identification and distribution of gene clusters

A genomic comparison was performed between genomes of strains exhibiting H_2-dependent formate production ($n = 12$) and those for which formate production was not detected ($n = 22$; Table S1). All formate producers had exclusively one and/or two complete specific gene clusters coding for an FHL1 and a putative formate dehydrogenase-NAD(P)H-oxidoreductase (Fdh-Nor), both annotated *fdh-mfh-mnh* and *fdh-nor*, respectively. These two clusters were composed of genes encoding formate dehydrogenase (*fdh*) and formate transporter (Fig. 2a), which seemed essential for H_2-dependent formate production.

The FHL1 cluster was previously described for *T. onnurineus* NA1 as 'the formate dehydrogenase operon' responsible for formate oxidation in the absence of H_2 in the culture at formate concentrations exceeding 1100 µM

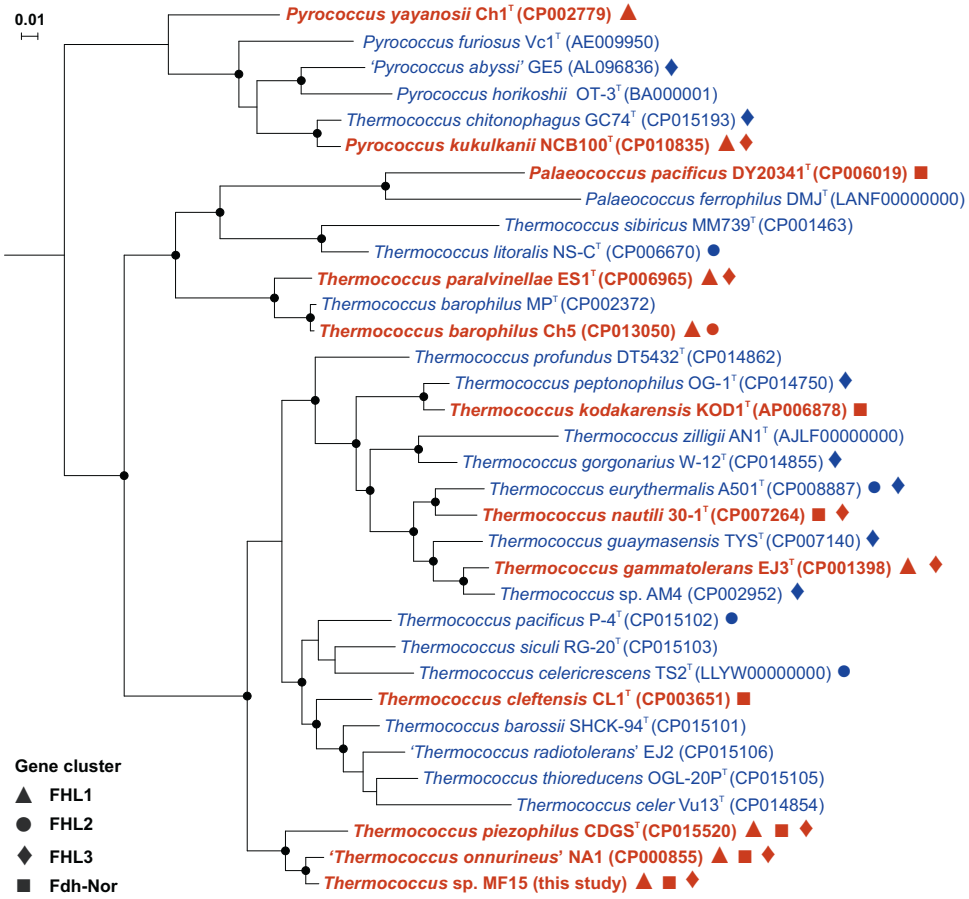

Fig. 1 Phylogenomic tree (based on 59 conserved archaeal marker proteins) representing H_2-tolerant *Thermococcales* capable of formate production in the absence of S^0. *Thermococcales* showing growth and production of formate in the presence of H_2 after 96 h of incubation are shown in bold and red, whereas H_2-sensitive strains are in blue. ASW medium contained: 30 mM bicarbonate, no S^0, 2 g L^{-1} yeast extract and H_2/CO_2 in headspace gas (80:20, v/v; 200 kPa). Incubation temperature was 80 °C for *Thermococcus* and *Palaeococcus* and 95 °C for *Pyrococcus*. Nodes with a bootstrap value >95% were marked in black solid dots. A black solid symbol indicated the presence in genomes of specific gene clusters: triangles for 'FHL1', circles for 'FHL2', diamonds for 'FHL3' and squares for 'Fdh-Nor'. GenBank accession numbers are given in brackets. Scale bar represents 0.01 substitutions per nucleotide position.

[21–23, 51]. This 17.1 kbp operon encompasses 18 genes coding for four subunit modules: a formate dehydrogenase (two genes, *fdh*), a group 4 membrane-bound [NiFe]-hydrogenase (eight genes, *mfh*) related to Complex I (NADH:ubiquinone oxidoreductase), a formate transporter (one gene) and a Na^+/H^+ antiporter (seven genes, *mnh*) [21] (Fig. 2a). However, here we identified a correlation between the presence of the FHL1 cluster and H_2-dependent formate production that disposes of reducing equivalents as previously suggested by Topçuoğlu and colleagues [20]. Moreover, further in silico genome analysis of *Thermococcales* also revealed the presence of numerous homologous nonspecific gene clusters (FHL2 and 3) in some strain genomes regardless of their capacity to produce formate (Fig. 2a and S1). Although these two gene clusters encoded homologous complexes of FHL1, proteins of the FHL2 were also quite divergent (average amino-acid sequence similarity of 39% with FHL1 of *T. onnurineus* NA1 TON_1563-80) and the gene coding for the formate transporter was systematically missing, suggesting again it was essential for the formate metabolism. In addition, the end of the FHL2 was also followed by a set of three genes (*nor*), encoding a putative cytoplasmic NAD(P)H-oxidoreductase, that were similar to the ones found in *fdh-nor* cluster (average amino-acid sequence similarity of 71% with the *fdh-nor* of *T. onnurineus* NA1 TON_0541-43, Fig. S1). Regarding the FHL3 cluster, it was partially present in fourteen strains as genes encoding Na^+/H^+ antiporter were specifically missing for seven strains (Figs.1 and 2a), which formed a tight phylogenetical cluster, suggesting their loss was related to a common ancestor. Moreover, an exclusive TetR/AcrR family transcriptional regulator was also present upstream of this cluster. Five of the complete FHL3-possessing strains could produce formate and also had the FHL1 cluster, suggesting that FHL3 had a different physiological function than FHL1.

Additional to the FHL1, a new cluster was also exclusively found in *Thermococcales* capable of H_2-dependent formate production (Figs. 1 and 2). This 5.5 kbp cluster was composed of three functional modules: a formate transporter (one gene), a formate dehydrogenase (two genes, *fdh*) and a putative cytoplasmic NAD(P)H-oxidoreductase (three genes, *nor*). Initially, the three-gene *nor* module was inferred to code for a putative glutamate synthase. Moreover, based on the cluster structures the Fdh-Nor cluster could be divided into two subgroup, Fdh-Nor1 and

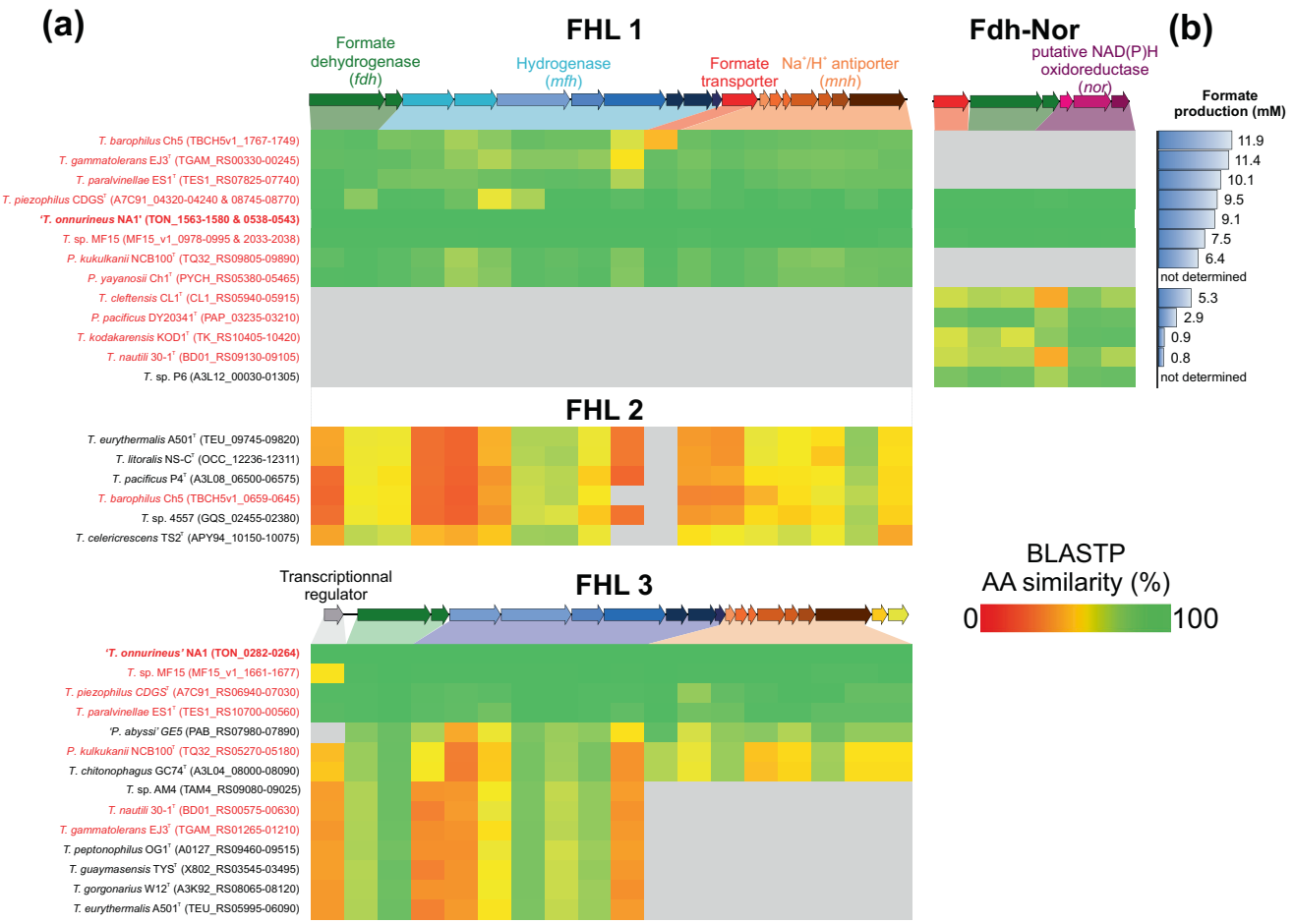

Fig. 2 Comparison of formate dehydrogenase containing gene clusters from 35 *Thermococcales* genomes sorted according to their H_2-dependent formate production. a Heat map showing similarity (blastp score) of each amino-acid (AA) sequence for *Thermococcales* compared with those of gene clusters from *T. onnurineus* NA1, which are represented above heat map (TON_1563-1580 for FHL1 and FHL2, TON_0282-0264 for FHL3 and TON_0538–0543 for Fdh-Nor). Grey squares indicate that no corresponding proteins were found. Gene clusters of *Thermococcales* that perform H_2-dependent formate production are indicated in red. GenBank accession numbers are given in brackets. **b** Formate production after 96 h of incubation in an ASW medium contained: 30 mM bicarbonate, H_2/CO_2 (80:20, v/v; 200 kPa) and 0.2 g L^{-1} yeast extract. *Thermococcus* and *Palaeococcus* were incubated at 80 °C and *Pyrococcus* at 95 °C. *Pyrococcus yayanosii* $Ch1^T$ and *T.* sp. P6 were not tested.

Fdh-Nor2 (Fig. S1). However, as several studies suggest, this module could in fact code for a putative cytoplasmic NAD(P)H-oxidoreductase [52–54] and therefore also represents a new pathway to discard electrons and dispose of reducing equivalents.

Putative evolutionary history

Although FHL-like complexes are found throughout the *Archaea* and *Bacteria* domains [55], these FHL-like clusters were almost specific to *Thermococcales* as the only known exception was found in *Thermofilum pendens* $Hrk5^T$ (Fig. S1), a *Crenarchaeota* also capable of sulfur respiration of peptides [56], which might have acquired this cluster through horizontal gene transfer. Among *Thermococcales*, the presence of multiple similar gene clusters reinforces the hypothesis that they could be remnants from a common ancestral cluster [57]. However, their evolutionary history remains unclear, and whether these genes were obtain by genetic transfer or lost through genetic drift [20], especially that the distribution of *Thermococcus* lineages may not follow a simple model of allopatric speciation [58]. Both FHL1 and Fdh-Nor gene clusters only co-occurred in the genomes of three formate producers (*T. onnurineus* NA1, *T. piezophilus* $CDGS^T$ and *T.* sp. MF15) that formed a tight phylogenomic cluster (Figs. 1 and 2a). These strains also showed a highly conserved (>95% amino-acid sequence similarity) gene cluster FHL3 (Fig. 2a). Moreover, sequence analysis of Fdh catalytic subunit and formate transporter showed two monophyletic groups (FHL1/Fdh-Nor1 and Fdh-Nor2, Fig. S2), suggesting a common evolutionary history as the current distribution of these two gene clusters

could be owing to initial horizontal transfers followed by a vertical inheritance.

Eleven *Thermococcales* also had two similar complexes to the FHL and Fdh-Nor with a carbon monoxide dehydrogenase as oxidoreductase instead of formate dehydrogenase (COdh-Mfh-Mnh and COdh-Nor) (Fig. S3). The COdh-Mfh-Mnh complex was previously described as involved in carboxidotrophic hydrogenogenic growth of *Thermococcus* ($CO + H_2O \rightarrow H_2 + CO_2$) [59], whereas the COdh-Nor complex seems to be involved in carboxidotrophic growth coupled to S^0 reduction in *Thermococcus gammatolerans* EJ3^T [51]. Moreover, three hydrogenogenic CO-oxidising *Thermococcus* (*T. barophilus* Ch5, *T. onnurineus* NA1 and *T. paralvinellae* ES1^T) have also the FHL1 cluster, which allows them to remove the H_2 and CO_2 produced through formate production, as *T. onnurineus* NA1 produced 5 mM of formate after 110 hours in the presence of CO in the gas phase ($CO/N_2/CO_2$, 50:30:20, v/v; 200 kPa). This suggests that H_2-dependent formate production could also act as a pathway for reducing-equivalents disposal in carboxidotrophic growth.

Function of the formate dehydrogenase, formate transporter and hydrogenases of the *fhl1* and *fdh-nor* clusters

All these gene clusters probably have different functions [57, 60], as suggested for *T. onnurineus* NA1, which possess three clusters including the *fhl1* and *fdh-nor* clusters. Gene expression of these different clusters varied according to the CO, formate and starch concentrations [21, 61–63], suggesting enzymes coded by these clusters could be specifically expressed in different environmental conditions. Moreover, although all *Thermococcales* with *fhl1* or *fdh-nor* clusters were tolerant to H_2 (Figs. 1 and 2), strains with the *fhl1* cluster had always produced more formate after 96 h (<11.9 mM for *T. barophilus* Ch5) than the four strains with only *fdh-nor* cluster (<5.3 mM for *Thermococcus cleftensis* CL1^T). However, production for the three strains with both clusters was not enhanced (from 7.5 to 9.5 mM) (Fig. 2). This discrepancy could be the consequence of the different pathways used by FHL1 and Fdh-Nor complexes to reduce CO_2 to formate.

In both FHL1 and Fdh-Nor, formate dehydrogenase (Fdh, 2 genes) and formate transporter (1 gene) proteins were conserved among strains as described in the previous section (Fig. 2 and S2). The Fdh catalyses the reduction of CO_2 as it was shown that the deletion of the catalytic subunit from the Fdh (TK_2076) of *fdh-nor* cluster in *T. kodakarensis* KOD1^T, disables formate production [64]. Moreover, H_2-dependent formate production was shown to be reversible in *T. onnurineus* NA1, *T. cleftensis* CL1^T and *Palaeococcus pacificus* DY20341^T depending on the ratio of formate and H_2 strongly suggesting that the reaction catalysed by FHL1 and Fdh-Nor complexes was bidirectional (Table S3).

The protein responsible for formate secretion was only found in *Thermococcales* and *Thermofilum pendens* Hrk5^T (Tpen_0191, Fig. S2) and therefore seems essential to H_2-dependent formate production. Protein TON_1573 was described as a formate transporter in *T. onnurineus* NA1 [21] that could be a formate-specific channel [55, 65]. Formate channels belong to the formate-nitrite transporters family and although functional mechanism of its members remains unclear, several studies suggested they function as specific bidirectional formate channels [66–68].

Besides the formate dehydrogenase and formate transporter, H_2-dependent formate production requires also a transfer, of the electrons generated through H_2 oxidation, to Fdh (Fig. 3). This could be performed by the Mfh complex (eight genes, 9.0 kbp) of the *fhl1* cluster or/and by the putative Nor complex (three genes, 1.9 kbp) of the *fdh-nor* cluster (Fig. 3). The function of this putative Nor complex, initially described as a glutamate synthase [69], remains controversial, and as several studies also suggest this complex could be an oxidoreductase [52–54]. Expression of the *fdh-nor* cluster in *T. onnurineus* NA1 is always correlated with the *sulf1* cluster encoding a NADPH-dependent cytosolic hydrogenase [61, 62, 70]. Hence, Fdh-Nor putative enzymatic complex could oxidise NADPH produced by the Sulf1 hydrogenase that reduces $NADP^+$ from H_2 oxidation and then transfers electrons to the Fdh for CO_2 reduction to formate (Fig. 3). Compared with the direct transfer of electrons from the Mfh complex to the Fdh, this different pathway encompasses additional intermediates that could lead to a lower yield in formate synthesis. This might explain why strains with only Fdh–Nor complex produce on average 25% less formate than strains with only FHL1 (Fig. 2).

H_2-dependent formate production: an alternative mechanism to S^0 reduction

Two different strains (MP^T and Ch5), both affiliated to *Thermococcus barophilus* [71, 72] had a different tolerance to H_2 in the absence of S^0 (Figs. 1 and 4). *T. barophilus* Ch5 presented growth with H_2, whereas *T. barophilus* MP^T was unable to grow at dissolved H_2 concentrations exceeding 0.8 µM. In order to understand why their tolerances to H_2 in the absence of S^0 were so different, the effect of different H_2 concentrations on growth of these two *T. barophilus* strains was compared with or without S^0 (Fig. 4). In the presence of S^0, cell growth of both strains after 24 hours of incubation was not affected by H_2 (Fig. 4a) as cell concentrations remained relatively constant at 3×10^8 cells mL^{-1} regardless of the initial H_2 concentration. In the absence of S^0, increasing H_2 partial pressures led to a total inhibition of

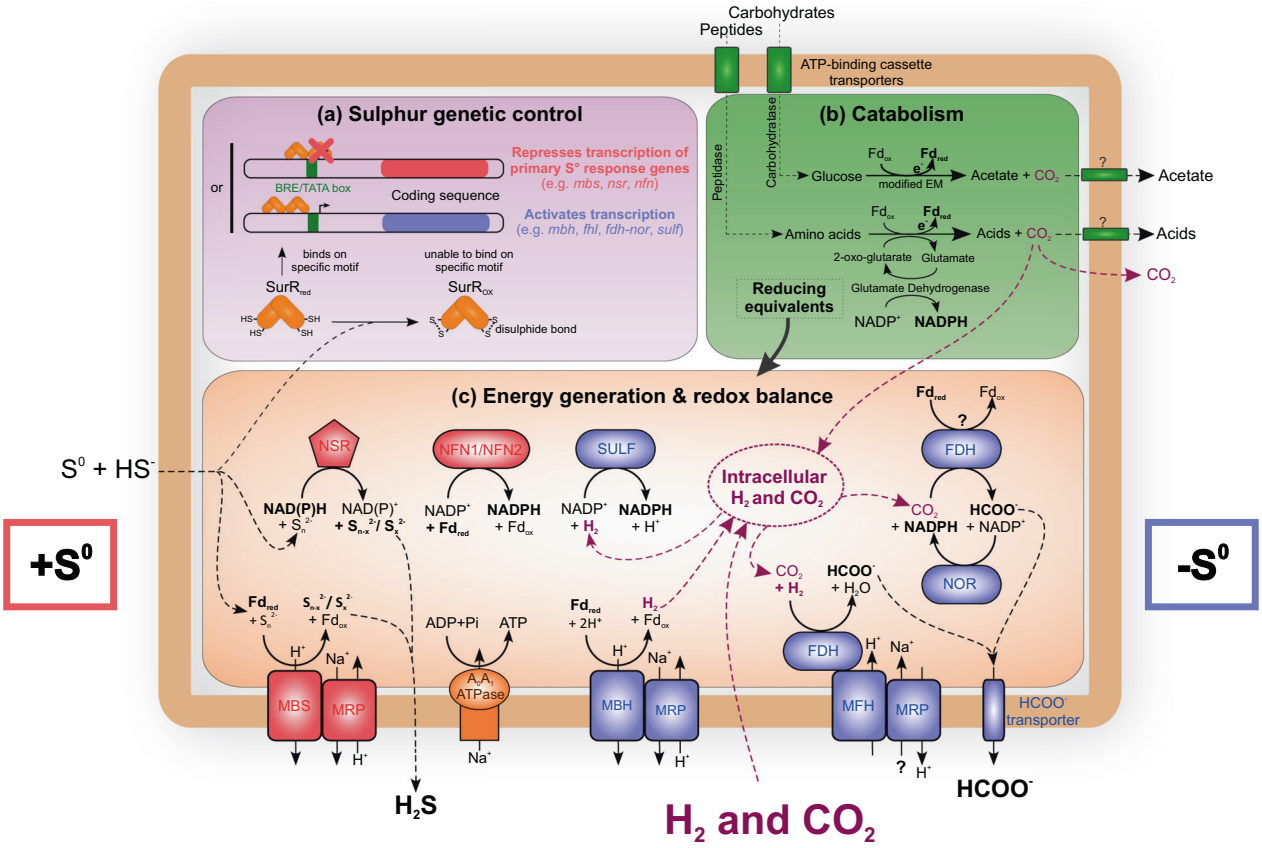

Fig. 3 Schematic representation of the metabolism of *Thermococcales* strains producing formate in the presence of H_2. Red and blue indicate proteins expressed prominently during growth in the presence or in absence of sulfur, respectively. Other proteins are designated by green and orange text. **a** Genetic control by sulfur (adapted from [10]); **b** Catabolism (transport and utilisation of carbohydrates and peptides); **c** Energy generation & redox balance. Most proteins indicated in this illustration are shared by the majority of *Thermococcales*. *BRE*, transcription factor B recognition element, *EM* Embden-Meyerhof, Fd_{ox} oxidised ferredoxin, Fd_{red} reduced ferredoxin, *fdh* formate dehydrogenase, *fhl* formate hydrogenlyase, *mbh* membrane-bound [NiFe]-hydrogenases, *mbs* membrane-bound sulfane reductase (previously known as '*mbx*' membrane-bound complex); *MFH* membrane-bound formate-dependent hydrogenase, *MRP* multiple resistance and pH antiporter, *NAD(P)* nicotinamide adenine dinucleotide (phosphate), *nfn* NADH-dependent ferredoxin $NADP^+$ oxidoreductase, *nor* NAD(P)H-oxidoreductase, *nsr* CoA-dependent NAD(P)H:sulfur oxidoreductase, *SULF* sulfhydrogenase; *SurR* sulfur response regulator. Diagram modified from [1, 20, 81, 82].

growth for strain MP^T at 0.8 mM of dissolved H_2 whereas growth of strain Ch5 was not affected by the increase in H_2 concentrations at 30 mM of bicarbonate (Fig. 4b). Furthermore, formate production was only observed for strain Ch5 (up to 5.7 mM) (Fig. 4d) and was correlated to the H_2 concentration ($R^2 = 0.99$, $p < 0.00001$). Although H_2-dependent formate production provided tolerance to H_2, this mechanism seemed not as efficient at 0.8 µM dissolved H_2 compared to S^0 reduction as there were on average 3.2-fold less cells for strain Ch5 in the absence of S^0 (Figs. 4a and 4b). So even in the absence of H_2 the presence of S^0 stimulated cell growth of strains MP^T and Ch5, suggesting that the yield and/or the kinetics of reducing-equivalents disposal were higher with S^0 than through H_2-dependent formate production.

In addition, CO_2 concentrations also had an effect on growth of both strains. CO_2 occurs at several levels of the catabolism of *Thermococcales* in peptides and pyruvate catabolism (e.g., [1]) but also in H_2-dependent formate production [20, 64]. In the presence of S^0 and regardless of the concentration of H_2, variation of bicarbonate concentrations did not notably affect the growth of these two strains (Fig. 4a), although acetate production systematically decreased as bicarbonate concentrations increased (Figs. 4f and 4e), strongly suggesting that the accumulation of CO_2 controlled thermodynamically the catabolism activity. In the absence of S^0, although growth of strain Ch5 (i.e., H_2-dependent formate producer) was also not affected by increasing H_2 concentrations at the highest bicarbonate concentration (30 mM), strain Ch5 growth decreased 2.8-fold (at 0.8 mM of dissolved H_2) simultaneously with the formate production (10.3-fold) as the bicarbonate concentration decreased from 30 to 2 mM (i.e., seawater concentration) (Figs. 4b and 4d). In contrast to strain Ch5, the increase of

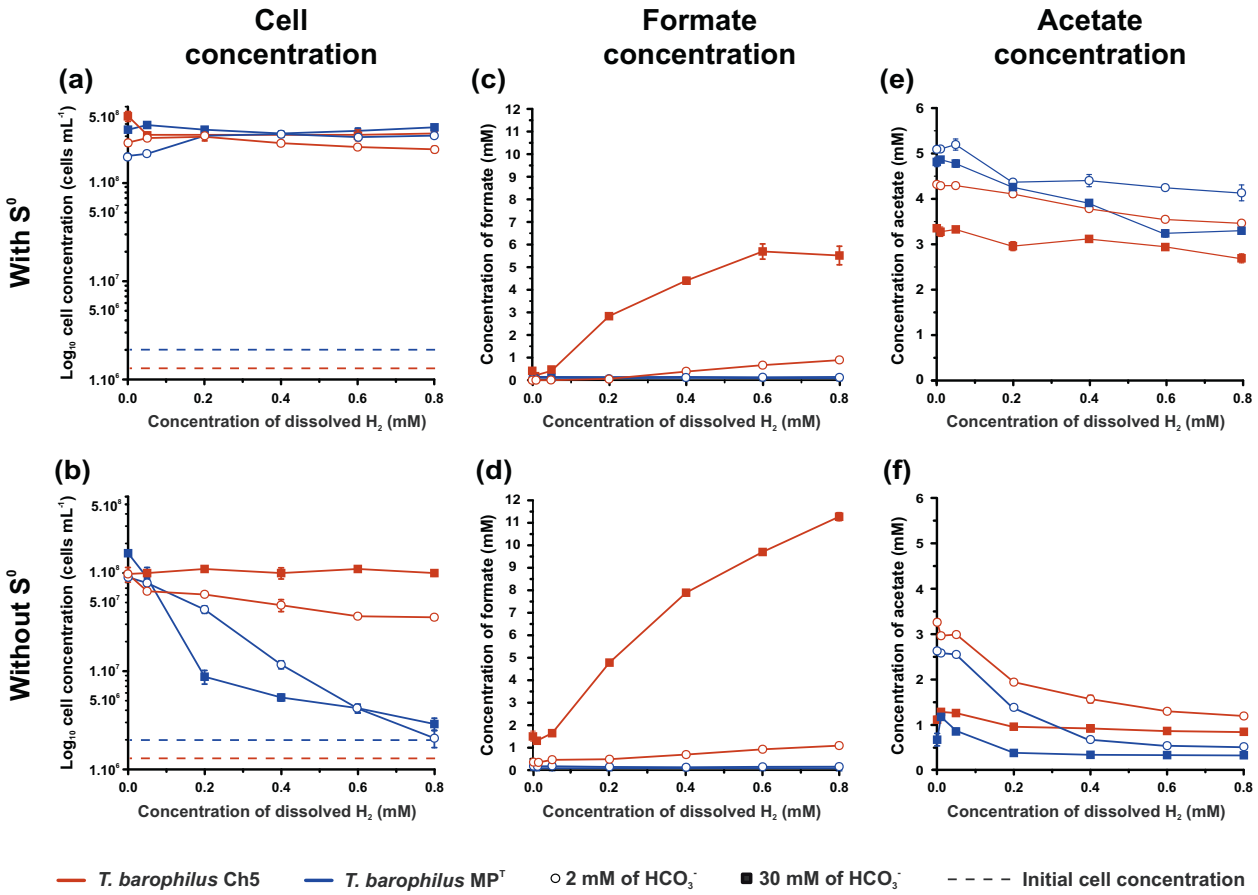

Fig. 4 Comparison of the effect of dissolved H_2 on growth, formate and acetate production after 48 h incubation of two strains of *Thermococcus barophilus* (MP^T and Ch5). In the presence (**a**, **c** and **e**) or in the absence (**b**, **c** and **f**) of 3 g L^{-1} of S^0 and at 2 or 30 mM of bicarbonate (empty dot and solid square, respectively). **a**, **b** Cell concentration. Dashed lines represent initial cell concentration before incubation. **c**, **d** Formate concentration. **e**, **f** Acetate concentration. *T. barophilus* Ch5 (red) can perform H_2-dependent formate whereas *T. barophilus* MP^T (blue) cannot. Cell concentrations and anion concentrations (formate and acetate) were measured after 24 and 48 h incubation, respectively at 80 °C in an ASW medium containing 2 g L^{-1} yeast extract. Effect of H_2 concentrations were examined in a range of 0–80% (v/v; 200 kPa; 0–0.8 mM dissolved H_2) with CO_2 concentrations kept at 20% (v/v). Error bars show standard error ($n = 3$).

bicarbonate concentrations seemed to limit the growth of strain MP^T in the absence of S^0, especially between 0.1 and 0.6 mM of dissolved H_2 (in average 3.5-fold decrease, Fig. 4b). This strongly suggests that not only H_2-dependent formate production coupled to CO_2 reduction controlled the tolerance of strain Ch5 to H_2 in the absence of S^0 but that CO_2 also enhanced strain Ch5 growth by improving H_2 removal.

Characterisation of H_2-dependent formate production

Formate oxidation ($HCOO^- + H_2O \rightarrow H_2 + HCO_3^-$) catalysed by formate dehydrogenase of the FHL1 complex is well studied in *Thermococcales* and more specifically in *T. onnurineus* NA1 [21–23, 62, 73]. However, the reverse reaction (i.e., H_2-dependent formate production) remains poorly characterised [20]. In order to confirm that bicarbonate reduction coupled to H_2 oxidation was responsible for the formate production in *Thermococcales*, *T. onnurineus* NA1 was incubated with ^{14}C-radiolabelled bicarbonate in the presence and in absence of H_2 (Fig. 5a). There was no ^{14}C-formate production neither in the abiotic control nor in the negative control (inoculated then autoclaved before incubation) and ^{14}C-formate production was only detected with viable cells in the presence of H_2, demonstrating that formate production was the result of H_2-oxidising bicarbonate reduction. In the presence of 0.8 mM of dissolved H_2 and 30 mM of bicarbonate, the maximum rate of formate production was in the same range (0.2 µmol cm^{-3} h^{-1}, 1.09 pmol $cell^{-1}$ h^{-1}, 56 µmol $hour^{-1}$ mg^{-1} of cells wet weight) as those obtained at 30 °C with *Acetobacterium woodii* (≈36 µmol $hour^{-1}$ mg^{-1} of cells wet weight) and at 60 °C with *Thermoanaerobacter kivui* (≈115 µmol $hour^{-1}$ mg^{-1} of cells wet weight) [26, 74]. As for *A. woodii*, formate accumulation increased in time and reached a plateau after 96 h (Fig. 5a), suggesting the reaction could have reached thermodynamic equilibrium.

In order to explore the possible thermodynamic control of the reaction, formate production was characterised for a range

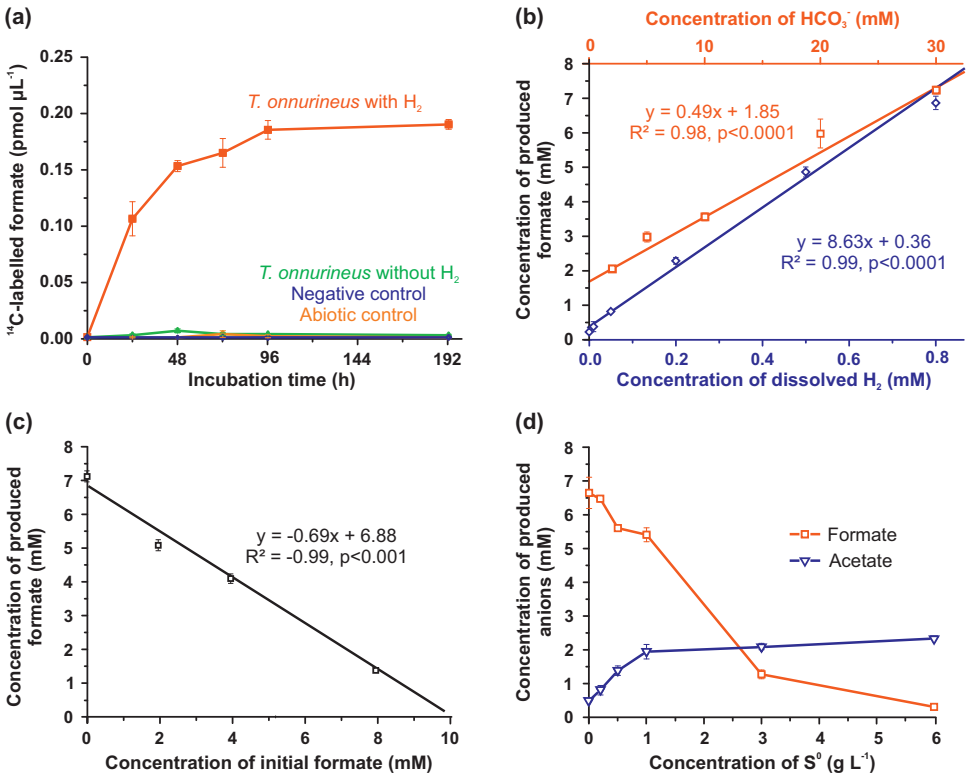

Fig. 5 Characterisation of H_2-dependent formate production of *T. onnurineus* NA1 at 80 °C. a Production of ^{14}C-formate from ^{14}C-bicarbonate (96 kBq) as a function of time. ASW medium contained: 30 mM bicarbonate, 0.2 g L^{-1} yeast extract, H_2/CO_2 or N_2/CO_2 headspace (80:20, v/v; 200 kPa) and no S^0 was added. Abiotic control was not inoculated. Negative control was autoclaved after inoculation (20 min at 121 °C). **b** Effect of dissolved H_2 (at 200 kPa) (blue diamonds) and bicarbonate (red spares) concentrations on formate production after 48 h incubation. ASW medium contained: 30 mM bicarbonate for H_2 experiments, H_2/CO_2 (80:20, v/v; 200 kPa) for bicarbonate experiments, all conditions 0.2 g L^{-1} yeast extract and no S^0 was added. **c** Effect of initial formate concentration on formate production after 192 h incubation. ASW medium contained: 30 mM bicarbonate, H_2/CO_2 (80:20, v/v; 200 kPa), 0.2 g L^{-1} yeast extract and no S^0 was added. **d** Effect of S^0 on formate (red squares) and acetate (blue triangles) productions after 384 h incubation. ASW medium contained: 30 mM bicarbonate, H_2/CO_2 (80:20, v/v; 200 kPa) and 2 g L^{-1} yeast extract. Error bars represent standard error ($n = 3$).

of substrate and product concentrations. Formate concentrations produced by *T. onnurineus* increased with increasing substrate concentrations as the formate production was positively and linearly correlated to dissolved H_2 and bicarbonate concentrations ($R^2 \geq 0.98$, $p < 0.0001$, Fig. 5b). Levels of formate production did not reach a plateau even at the highest H_2 and bicarbonate concentrations tested (0.8 and 30 mM, respectively), suggesting that formate production per cell could be enhanced at higher dissolved H_2 concentrations. In culture, formate accumulation was the most limiting factor as formate production was negatively correlated with the initial concentration of formate ($R^2 = 0.99$, $P < 0.001$, Fig. 5c) and was inhibited at formate concentrations >9.9 mM in the presence of 0.8 mM of dissolved H_2 and 30 mM of bicarbonate (Fig. 5c). Interestingly, with bicarbonate in the range of seawater concentrations (i.e., 2 mM) and with moderate concentrations of dissolved H_2, compared with those usually detected in deep-sea hydrothermal fluids (i.e., 0.8 mM), formate production was inhibited at the higher formate concentrations (1077 µM, Fig. S4) in regard to the highest levels detected in these environments (e.g., 158 µmol kg^{-1} of hydrothermal fluid for Lost City) [75]. Hence, although thermodynamic constraints strongly controlled H_2-dependent formate production, our experimental data suggest that environmental formate concentrations should not limit formate production in most of the hydrothermal habitats described so far.

In addition, effects of S^0 were also assessed as H_2-dependent formate production is an alternative pathway to S^0 reduction for reducing-equivalents disposal. An increase in S^0 concentrations stimulated *T. onnurineus* NA1 catabolic activity as acetate, one of the main final fermentation products of *Thermococcales* [1], increased simultaneously levelling out towards a maximum over 1 g L^{-1} (31.2 mM) of S^0 (Fig. 5d). This S^0 threshold over which the catabolism was not further stimulated could either suggest that electron donors or accessibility to S^0 became limited (especially that cultures were not shaken), or that the reaction reached the maximal velocity or that the SurR system was saturated [11]. However, maximum S^0 concentrations measured in situ were three orders of magnitude lower than the lowest

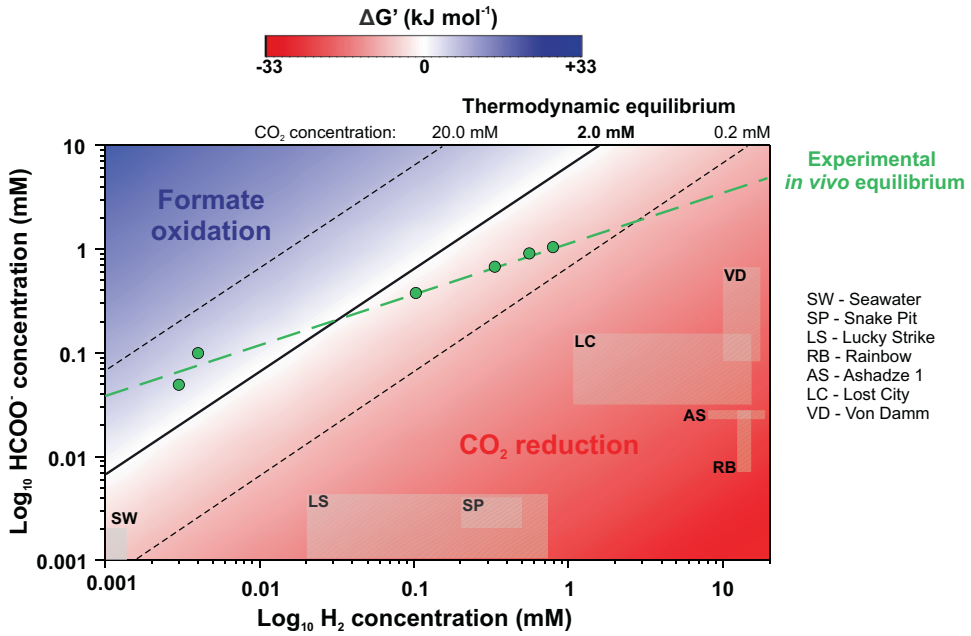

Fig. 6 The direction of the reaction of CO_2 reduction depends primarily on substrate concentration. 2D-contour plot representing the thermodynamic modelling of the CO_2 reduction to formate for a range of concentrations of formate and H_2. Gibbs free energy of the reaction ($H_{2\,(g)}+HCO_3^-{}_{(aq)} \rightarrow HCOO^-{}_{(aq)}+H_2O_{(l)}$) was calculated for 80 °C and 2 mM of bicarbonate. As H_2 was assumed as a gaseous substrate for ΔG' calculations, H_2 partial pressures were converted to dissolved concentrations to compare with all the experimental and in situ data. The blue area indicates conditions for which formate oxidation occurs, whereas the red area indicates conditions for which CO_2 reduction to formate occurs. The black solid line and dashed lines define points of the chemical equilibrium of the reaction ($\Delta G' = 0\,kJ\,mol^{-1}$) from thermodynamic modelling for three different bicarbonate concentrations, 2.0 mM, 0.2 mM, and 20.0 mM, respectively. The Green dashed line defines the experimental in vivo point of the chemical equilibrium of the reaction measured for *T. onnurineus* NA1 in culture medium after 96 h of incubation at 80 °C (see details Fig. S4). Effect of H_2 concentrations were examined in a range of 0–80% (v/v; 200 kPa; 0–0.8 mM dissolved H_2) with CO_2 concentrations kept at 20% (v/v). The effect of formate concentrations was examined in a range of 0 to 1 mM. ASW medium contained: 2 mM bicarbonate, 0.2 g L^{-1} yeast extract and no S^0 was added. Grey squares represent environmental concentrations measured for seawater and six hydrothermal vent fields (data available in Table S4).

S^0 concentration over which the catabolism was not further stimulated [48, 50, 76]. At this in situ S^0 concentration (<33 µM) [48–50], *T. onnurineus* NA1 would theoretically only exhibit 21% of the maximum acetate production, which is only 0.07% more than without S^0, suggesting that the use by *Thermococcales* of the S^0 reduction pathway could be limited in hydrothermal ecosystems as disposal of reducing equivalents through this pathway would be negligible compared to H_2-dependent formate production. Moreover, conversely to the S^0 reduction pathway, formate production was inhibited by increasing S^0 concentration especially at higher bicarbonate concentrations (Figs. 5d, 4c, d). This result was also consistent with the inhibition of the formate oxidation catabolic reaction [21] and with the fact that H_2-dependent formate production is also regulated by the accessibility to S^0. Thus, *Thermococcales* probably save energy by only keeping one active electron discard pathway, depending mainly on the environmental sulfur availability. However, at in situ S^0 concentrations and in the presence of H_2, it remains unclear if both electron discard pathways to dispose of reducing equivalents remain active.

In situ reduction of carbon dioxide to formate

It has been demonstrated that *Thermococcales* conserved energy from formate oxidation at high formate concentrations (1.1–150 mM) in pure culture [21, 22], although it remains unclear whether cell growth solely relies on formate oxidation or if the yeast extract present in the medium also contributes to growth [24]. Moreover, in most hydrothermal environments, where levels of available S^0 are not sufficient to efficiently dispose of reducing equivalents, it also remains uncertain whether formate oxidation occurs in situ as suggested in some studies [20, 22, 51]. Although the Gibbs free energy (ΔG^0) of the H_2-dependent CO_2 reduction to formate is almost at equilibrium ($-1.5\,kJ\,mol^{-1}$) in standard conditions considering H_2 as gas [77], it can reach $-19\,kJ\,mol^{-1}$ if H_2 is considered as dissolved in the aqueous phase.

Here, we show using thermodynamic modelling and experimental data from cultures of *T. onnurineus* NA1 for a wide range of H_2 (assumed as gas or dissolved) and formate concentrations representative of those found in deep-sea hydrothermal systems [75, 78, 79] (Table S4), that only H_2-

dependent CO_2 reduction to formate occurred in these conditions (Fig. 6, S4–6), and even at hydrothermal sites for which formate oxidation was the most favourable. For example, using bicarbonate concentration similar to that of seawater (*i.e.* 2 mM) and in situ hydrothermal fluid H_2 concentrations for Lost City and Von Damm, the only known hydrothermal vent fields at which formate concentrations exceed 100 µM [75, 79], CO_2 reduction to formate was still thermodynamically more favourable (ΔG' between −13.4 and −21.4 kJ mol^{-1}) (Fig. 6). As formate oxidation by *Thermococcales* is probably encountered rarely in hydrothermal environments, the FHL1 and Fdh-Nor complexes mainly perform H_2-dependent CO_2 reduction to formate as an alternative pathway to sulfur reduction for electrons disposal. Moreover, H_2-dependent formate rates remain elevated beyond at least 5 °C over and below the temperature range for growth of *T. onnurineus* NA1, suggesting that the reaction could be maintained in cooler ecological niches ($Ea = 28{,}6$ kJ mol^{-1}; Q_{10} (75;85 °C) = 1.318; Fig. S7). Given the ubiquity of *Thermococcales* in marine ecosystems (e.g. [80]), chemolithotrophic H_2-dependent formate production could play a role in the distribution of these microbial communities and on larger scales impact the organic carbon balance and the carbon cycle in the deep ocean.

Acknowledgements The authors thank Christophe Brandily, Françoise Lesongeur and Nadège Quintin for technical support, and Yves Fouquet, Karine Alain, Mohamed Jebbar, Jordan Hartunians and Jean-Pierre Donval for useful discussions. We are much indebted to anonymous referees for their helpful comments. We also thank Cécile Cathalot for providing hydrothermal fluid samples and Marie-Anne Cambon-Bonavita, chief scientist of BICOSE 1 and 2 cruises. All crew members and the Scientific Party were crucial in this effort, especially the ROV '*Victor 6000*' and DSV '*Nautile*' crews for the sampling efforts. Sébastien Le Guellec was supported by the 'Laboratoire d'Excellence' LabexMER (ANR-10-LABX-19) and co-funded by a grant from Ifremer and the Regional Council of Brittany. Elodie Leroy was supported by a grant from Ifremer.

Compliance with ethical standards

Conflict of interest The authors declare no competing interest.

Publisher's note Springer Nature remains neutral with regard to jurisdictional claims in published maps and institutional affiliations.

References

1. Schut GJ, Lipscomb GL, Han Y, Notey JS, Kelly RM, Adams MWW. The order *Thermococcales* and the family *Thermococcaceae*. In: Rosenberg E (ed). The Prokaryotes: Other Major Lineages of *Bacteria* and the *Archaea*. 4th edn. (Springer-Verlag, 2014) pp 363–83.
2. Zillig W, Holz I, Janekovic D, Schäfer W, Reiter WD. The Archaebacterium *Thermococcus celer* Represents, a Novel Genus within the Thermophilic Branch of the *Archaebacteria*. Syst Appl Microbiol. 1983;4:88–94.
3. Fiala G, Stetter KO. *Pyrococcus furiosus* sp. nov. represents a novel genus of marine heterotrophic archaebacteria growing optimally at 100°C. Arch Microbiol. 1986;145:56–61.
4. Takai K, Sugai A, Itoh T, Horikoshi K. *Palaeococcus ferrophilus* gen. nov., sp. nov., a barophilic, hyperthermophilic archaeon from a deep-sea hydrothermal vent chimney. Int J Syst Evol Microbiol. 2000;50:489–500.
5. Sokolova TG, Jeanthon C, Kostrikina NA, Chernyh NA, Lebedinsky AV, Stackebrandt E, et al. The first evidence of anaerobic CO oxidation coupled with H_2 production by a hyperthermophilic archaeon isolated from a deep-sea hydrothermal vent. Extremophiles. 2004;8:317–23.
6. Bae SS, Kim TW, Lee HS, Kwon KK, Kim YJ, Kim M-S, et al. H_2 production from CO, formate or starch using the hyperthermophilic archaeon, *Thermococcus onnurineus*. Biotechnol Lett. 2012;34:75–9.
7. Pisa KY, Huber H, Thomm M, Müller V. A sodium ion-dependent A_1A_O ATP synthase from the hyperthermophilic archaeon *Pyrococcus furiosus*. FEBS J. 2007;274:3928–38.
8. Mayer F, Lim JK, Langer JD, Kang SG, Müller V. Na^+ transport by the A_1A_O-ATP synthase purified from *Thermococcus onnurineus* and reconstituted into liposomes. J Biol Chem. 2015;290:6994–7002.
9. Lipscomb GL, Keese AM, Cowart DM, Schut GJ, Thomm M, Adams MWW, et al. SurR: a transcriptional activator and repressor controlling hydrogen and elemental sulfur metabolism in *Pyrococcus furiosus*. Mol Microbiol. 2009;71:332–49.
10. Yang H, Lipscomb GL, Keese AM, Schut GJ, Thomm M, Adams MWW, et al. SurR regulates hydrogen production in *Pyrococcus furiosus* by a sulfur-dependent redox switch. Mol Microbiol. 2010;77:1111–22.
11. Lipscomb GL, Schut GJ, Scott RA, Adams MWW. SurR is a master regulator of the primary electron flow pathways in the order *Thermococcales*. Mol Microbiol. 2017;104:869–81.
12. Ma K, Schicho RN, Kelly RM, Adams MWW. Hydrogenase of the hyperthermophile *Pyrococcus furiosus* is an elemental sulfur reductase or sulfhydrogenase: evidence for a sulfur-reducing hydrogenase ancestor. Proc Natl Acad Sci USA. 1993;90:5341–4.
13. Wu C-H, Schut GJ, Poole FL, Haja DK, Adams MWW. Characterization of membrane-bound sulfane reductase: a missing link in the evolution of modern day respiratory complexes. J Biol Chem. 2018;293:16687–96.
14. Sapra R, Verhagen MFJM, Adams MWW. Purification and Characterization of a Membrane-Bound Hydrogenase from the Hyperthermophilic Archaeon *Pyrococcus furiosus*. J Bacteriol. 2000;182:3423–8.
15. Sapra R, Bagramyan K, Adams MWW. A simple energy-conserving system: Proton reduction coupled to proton translocation. Proc Natl Acad Sci USA. 2003;100:7545–50.
16. Bonch-Osmolovskaya E, Stetter K. Interspecies hydrogen transfer in cocultures of thermophilic. Archaea Syst Appl Microbiol. 1991;14:205–8.
17. Malik B, Su WW, Wald H, et al. R. Growth and gas production for hyperthermophilic archaebacterium, *Pyrococcus furiosus*. Biotechnol Bioeng. 1989;34:1050–7.
18. Schäfer T, Schönheit P. Pyruvate metabolism of the hyperthermophilic archaebacterium *Pyrococcus furiosus*. Arch Microbiol. 1991;155:366–77.
19. Dalmasso C, Oger P, Selva G, Courtine D, L'Haridon S, Garlaschelli A, et al. *Thermococcus piezophilus* sp. nov., a novel hyperthermophilic and piezophilic archaeon with a broad pressure range for growth, isolated from a deepest hydrothermal vent at the Mid-Cayman Rise. Syst Appl Microbiol. 2016;39:440–4.
20. Topçuoğlu BD, Meydan C, Orellana R, Holden JF. Formate hydrogenlyase and formate secretion ameliorate H_2 inhibition in the hyperthermophilic archaeon *Thermococcus paralvinellae*. Environ Microbiol. 2018;20:949–57.

21. Kim YJ, Lee HS, Kim ES, Bae SS, Lim JK, Matsumi R, et al. Formate-driven growth coupled with H_2 production. Nature. 2010;467:352.
22. Lim JK, Bae SS, Kim TW, Lee J-H, Lee HS, Kang SG. Thermodynamics of formate-oxidizing metabolism and implications for H_2 production. Appl Environ Microbiol. 2012;78:7393–7.
23. Lim JK, Mayer F, Kang SG, Müller V. Energy conservation by oxidation of formate to carbon dioxide and hydrogen via a sodium ion current in a hyperthermophilic archaeon. Proc Natl Acad Sci USA. 2014;111:11497–502.
24. Müller V, Hess V. The minimum biological energy quantum. Front Microbiol. 2017;8:2019.
25. Woods DD. Hydrogenlyases: the synthesis of formic acid by bacteria. Biochem J. 1936;30:515.
26. Schuchmann K, Müller V. Direct and reversible hydrogenation of CO_2 to formate by a bacterial carbon dioxide reductase. Science. 2013;342:1382–5.
27. Alissandratos A, Kim H-K, Easton CJ. Formate production through carbon dioxide hydrogenation with recombinant whole cell biocatalysts. Bioresour Technol. 2014;164:7–11.
28. Cambon-Bonavita M-A BICOSE cruise, RV Pourquoi pas?. Cruise Report. 2014; https://doi.org/10.17600/18000004.
29. Widdel F, Kohring GW, Mayer F. Studies on dissimilatory sulfate-reducing bacteria that decompose fatty acids. Arch Microbiol. 1983;134:286–94.
30. Widdel F, Bak F Gram-negative mesophilic sulfate-reducing bacteria. In: Balows A, Trüper HG, Dworkin M, Harder W, Schleifer KH (eds). The Prokaryotes. (Springer, 1992) pp 3352–78.
31. Bae S-S, Kim Y-J, Yang S-H, Lim J-K, Jeon J-H, Lee H-S, et al. *Thermococcus onnurineus* sp. nov., a hyperthermophilic archaeon isolated from a deep-sea hydrothermal vent area at the PACMANUS field. J. Microbiol. Biotechnol. 2006;16:1826–31.
32. Roussel EG, Cragg BA, Webster G, Sass H, Tang X, Williams AS, et al. Complex coupled metabolic and prokaryotic community responses to increasing temperatures in anaerobic marine sediments: critical temperatures and substrate changes. FEMS Microbiol Ecol. 2015;91:fiv084.
33. Rinke C, Schwientek P, Sczyrba A, Ivanova NN, Anderson IJ, Cheng J-F, et al. Insights into the phylogeny and coding potential of microbial dark matter. Nature. 2013;499:431.
34. Katoh K, Standley DM. MAFFT multiple sequence alignment software version 7: improvements in performance and usability. Mol Biol Evol. 2013;30:772–80.
35. Criscuolo A, Gribaldo S. BMGE (Block Mapping and Gathering with Entropy): a new software for selection of phylogenetic informative regions from multiple sequence alignments. BMC Evol Biol. 2010;10:210.
36. Gouy M, Guindon S, Gascuel O. SeaView version 4: a multiplatform graphical user interface for sequence alignment and phylogenetic tree building. Mol Biol Evol. 2009;27:221–4.
37. Guindon S, Dufayard J-F, Lefort V, Anisimova M, Hordijk W, Gascuel O. New algorithms and methods to estimate maximum-likelihood phylogenies: assessing the performance of PhyML 3.0. Syst Biol. 2010;59:307–21.
38. Lefort V, Longueville J-E, Gascuel O. SMS: smart model selection in PhyML. Mol Biol Evol. 2017;34:2422–4.
39. Le SQ, Gascuel O. An improved general amino acid replacement matrix. Mol Biol Evol. 2008;25:1307–20.
40. Blom J, Kreis J, Spänig S, Juhre T, Bertelli C, Ernst C, et al. EDGAR 2.0: an enhanced software platform for comparative gene content analyses. Nucleic Acids Res. 2016;44:W22–W8.
41. Oberto J. SyntTax: a web server linking synteny to prokaryotic taxonomy. BMC Bioinformatics. 2013;14:4.
42. Wagman DD, Evans WH, Parker VB, Schumm RH, Halow I. The NBS tables of chemical thermodynamic properties. Selected values for inorganic and C_1 and C_2 organic substances in SI units. J Phys Chem Ref Data. 1982;18:1807–18.
43. Amend et LaRowe Amend JP, LaRowe DE. Minireview: demystifying microbial reaction energetics. Environ Microbiol. 2019;21:3539–47.
44. Aller R, Yingst J. Relationships between microbial distributions and the anaerobic decomposition of organic matter in surface sediments of Long Island Sound, USA. Mar Biol. 1980;56:29–42.
45. Wiesenburg DA, Guinasso NL Jr. Equilibrium solubilities of methane, carbon monoxide, and hydrogen in water and sea water. J Chem Eng Data. 1979;24:356–60.
46. Weiss RF. The solubility of nitrogen, oxygen and argon in water and seawater. Deep-Sea Res Oceanogr Abstr. 1970;17:721. 35
47. McDermott JM, Sylva SP, Ono S, German CR, Seewald JS. Geochemistry of fluids from Earth's deepest ridge-crest hot-springs: Piccard hydrothermal field, Mid-Cayman Rise. Geochim Cosmochim Acta. 2018;228:95–118.
48. Rozan TF, Theberge S, Luther G III. Quantifying elemental sulfur (S0), bisulfide (HS^-) and polysulfides (S_x^{2-}) using a voltammetric method. Anal Chim Acta. 2000;415:175–84.
49. Luther GW III, Glazer BT, Hohmann L, Popp JI, Taillefert M, Rozan TF, et al. Sulfur speciation monitored in situ with solid state gold amalgam voltammetric microelectrodes: polysulfides as a special case in sediments, microbial mats and hydrothermal vent waters. J Environ Monit. 2001;3:61–6.
50. Findlay AJ, Gartman A, MacDonald DJ, Hanson TE, Shaw TJ, Luther GW III. Distribution and size fractionation of elemental sulfur in aqueous environments: the Chesapeake Bay and Mid-Atlantic Ridge. Geochim Cosmochim Acta. 2014;142:334–48.
51. Kozhevnikova D, Taranov E, Lebedinsky A, Bonch-Osmolovskaya E, Sokolova T. Hydrogenogenic and sulfidogenic growth of *Thermococcus* archaea on carbon monoxide and formate. Microbiology. 2016;85:400–10.
52. Schut GJ, Brehm SD, Datta S, Adams MWW, Whole-genome DNA. microarray analysis of a hyperthermophile and an archaeon: *Pyrococcus furiosus* grown on carbohydrates or peptides. J Bacteriol. 2003;185:3935–47.
53. Stutz HE, Reid SJ. GltX from *Clostridium saccharobutylicum* NCP262: glutamate synthase or oxidoreductase? Biochim Biophys Acta-Gene Regul Mech. 2004;1676:71–82.
54. Dincturk HB, Cunin R, Akce H. Expression and functional analysis of glutamate synthase small subunit-like proteins from archaeon *Pyrococcus horikoshii*. Microbiol Res. 2011;166:294–303.
55. Pinske C, Sargent F. Exploring the directionality of *Escherichia coli* formate hydrogenlyase: a membrane-bound enzyme capable of fixing carbon dioxide to organic acid. Microbiologyopen. 2016;5:721–37.
56. Zillig W, Gierl A, Schreiber G, Wunderl S, Janekovic D, Stetter K, et al. The archaebacterium *Thermofilum pendens* represents, a novel genus of the thermophilic, anaerobic sulfur respiring *Thermoproteales*. Syst Appl Microbiol. 1983;4:79–87.
57. Schut GJ, Boyd ES, Peters JW, Adams MWW. The modular respiratory complexes involved in hydrogen and sulfur metabolism by heterotrophic hyperthermophilic *archaea* and their evolutionary implications. FEMS Microbiol Rev. 2013;37:182–203.
58. Price MT, Fullerton H, Moyer CL. Biogeography and evolution of *Thermococcus* isolates from hydrothermal vent systems of the Pacific. Front Microbiol. 2015;6:968.
59. Lee HS, Kang SG, Bae SS, Lim JK, Cho Y, Kim YJ, et al. The complete genome sequence of *Thermococcus onnurineus* NA1 reveals a mixed heterotrophic and carboxydotrophic metabolism. J Bacteriol. 2008;190:7491–9.
60. Lim JK, Kang SG, Lebedinsky AV, Lee J-H, Lee HS. Identification of a novel class of membrane-bound [NiFe]-hydrogenases

in *Thermococcus onnurineus* NA1 by *in silico* analysis. Appl Environ Microb. 2010;76:6286–9.
61. Yun S-H, Kwon SO, Park GW, Kim JY, Kang SG, Lee J-H, et al. Proteome analysis of *Thermococcus onnurineus* NA1 reveals the expression of hydrogen gene cluster under carboxydotrophic growth. J Proteomics. 2011;74:1926–33.
62. Moon Y-J, Kwon J, Yun S-H, Lim HL, Kim M-S, Kang SG, et al. Proteome analyses of hydrogen-producing hyperthermophilic archaeon *Thermococcus onnurineus* NA1 in different one-carbon substrate culture conditions. Mol Cell Proteomics. 2012;11:M111. 015420
63. Kim M-S, Bae SS, Kim YJ, Kim TW, Lim JK, Lee SH, et al. CO-dependent H_2 production by genetically engineered *Thermococcus onnurineus* NA1. Appl Environ Microb. 2013;79:2048–53.
64. Nohara K, Orita I, Nakamura S, Imanaka T, Fukui T. Genetic examination and mass balance analysis of pyruvate/amino acid oxidation pathways in the hyperthermophilic archaeon *Thermococcus kodakarensis*. J Bacteriol. 2014;196:3831–9.
65. Lipscomb GL, Schut GJ, Thorgersen MP, Nixon WJ, Kelly RM, Adams MWW. Engineering hydrogen gas production from formate in a hyperthermophile by heterologous production of an 18-subunit membrane-bound complex. J Biol Chem. 2014;289:2873–9.
66. Suppmann B, Sawers G. Isolation and characterization of hypophosphite-resistant mutants of *Escherichia coli*: identification of the FocA protein, encoded by the *pfl* operon, as a putative formate transporter. Mol Microbiol. 1994;11:965–82.
67. Wang Y, Huang Y, Wang J, Cheng C, Huang W, Lu P, et al. Structure of the formate transporter FocA reveals a pentameric aquaporin-like channel. Nature. 2009;462:467.
68. Falke D, Schulz K, Doberenz C, Beyer L, Lilie H, Thiemer B, et al. Unexpected oligomeric structure of the FocA formate channel of *Escherichia coli*: a paradigm for the formate–nitrite transporter family of integral membrane proteins. FEMS Microbiol Lett. 2010;303:69–75.
69. Jongsareejit B, Rahman R, Fujiwara S, Imanaka T. Gene cloning, sequencing and enzymatic properties of glutamate synthase from the hyperthermophilic archaeon *Pyrococcus* sp. KOD1. Mol Gen Genet. 1997;254:635–42.
70. Lee SH, Kim M-S, Kim YJ, Kim TW, Kang SG, Lee HS. Transcriptomic profiling and its implications for the H_2 production of a non-methanogen deficient in the frhAGB-encoding hydrogenase. Appl Microbiol Biotechnol. 2017;101:5081–8.
71. Marteinsson VT, Birrien J-L, Reysenbach A-L, Vernet M, Marie D, Gambacorta A, et al. *Thermococcus barophilus* sp. nov., a new barophilic and hyperthermophilic archaeon isolated under high hydrostatic pressure from a deep-sea hydrothermal vent. Int J Syst Evol Microbiol. 1999;49:351–9.
72. Oger P, Sokolova TG, Kozhevnikova DA, Taranov EA, Vannier P, Lee HS, et al. Complete genome sequence of the hyperthermophilic and piezophilic archaeon *Thermococcus barophilus* Ch5, capable of growth at the expense of hydrogenogenesis from carbon monoxide and formate. Genome Announc. 2016;4:e01534–15.
73. Takács M, Tóth A, Bogos B, Varga A, Rákhely G, Kovács KL. Formate hydrogenlyase in the hyperthermophilic archaeon, *Thermococcus litoralis*. BMC Microbiol. 2008;8:88.
74. Schwarz FM, Müller V. Whole-cell biocatalysis for hydrogen storage and syngas conversion to formate using a thermophilic acetogen. Biotechnol Biofuels. 2020;13:1–11.
75. Lang SQ, Butterfield DA, Schulte M, Kelley DS, Lilley MD. Elevated concentrations of formate, acetate and dissolved organic carbon found at the Lost City hydrothermal field. Geochim Cosmochim Acta. 2010;74:941–52.
76. Breier J, Toner BM, Fakra S, Marcus M, White S, Thurnherr A, et al. Sulfur, sulfides, oxides and organic matter aggregated in submarine hydrothermal plumes at 9 50′ N East Pacific Rise. Geochim Cosmochim Acta. 2012;88:216–36.
77. Schuchmann K, Müller V. Autotrophy at the thermodynamic limit of life: a model for energy conservation in acetogenic bacteria. Nat Rev Microbiol. 2014;12:809.
78. Charlou JL, Donval JP, Konn C, Ondréas H, Fouquet Y, Jean-Baptiste P, et al. High production and fluxes of H_2 and CH_4 and evidence of abiotic hydrocarbon synthesis by serpentinization in ultramafic-hosted hydrothermal systems on the Mid-Atlantic Ridge. In: Rona PA, Devey CW, Dyment J, Murton BJ (eds). Diversity of hydrothermal systems on slow spreading ocean ridges. (John Wiley & Sons, 2010) pp 265–96.
79. McDermott JM, Seewald JS, German CR, Sylva SP. Pathways for abiotic organic synthesis at submarine hydrothermal fields. Proc Natl Acad Sci USA. 2015;112:7668–72.
80. Orcutt BN, Sylvan JB, Knab NJ, Edwards KJ. Microbial ecology of the dark ocean above, at, and below the seafloor. Microbiol Mol Biol Rev. 2011;75:361–422.
81. Mardanov AV, Ravin NV, Svetlitchnyi VA, Beletsky AV, Miroshnichenko ML, Bonch-Osmolovskaya EA, et al. Metabolic versatility and indigenous origin of the archaeon *Thermococcus sibiricus*, isolated from a siberian oil reservoir, as revealed by genome analysis. Appl Environ Microb. 2009;75:4580–8.
82. Proskurowski G, Lilley MD, Seewald JS, Früh-Green GL, Olson EJ, Lupton JE, et al. Abiogenic hydrocarbon production at Lost City hydrothermal field. Science. 2008;319:604–7.